Available online at www.sciencedirect.com
ScienceDirect
Bioorganic & Medicinal Chemistry 16 (2008) 5606–5618
Bioorganic & Medicinal Chemistry

Pharmacological and pharmacokinetic characterization of 2-piperazine-α-isopropyl benzylamine derivatives as melanocortin-4 receptor antagonists

Chen Chen,[a,*] Fabio C. Tucci,[a,†] Wanlong Jiang,[a] Joe A. Tran,[a] Beth A. Fleck,[b] Sam R. Hoare,[b] Jenny Wen,[c] Takung Chen,[c] Michael Johns,[c] Stacy Markison,[d] Alan C. Foster,[d] Dragan Marinkovic,[a] Caroline W. Chen,[a] Melissa Arellano,[a] John Harman,[a] John Saunders,[a,‡] Haig Bozigian[e] and Daniel Marks[e]

[a]*Department of Medicinal Chemistry, Neurocrine Biosciences, Inc., 12790 El Camino Real, San Diego, CA 92130, USA*
[b]*Department of Pharmacology, Neurocrine Biosciences, Inc., 12790 El Camino Real, San Diego, CA 92130, USA*
[c]*Department of Preclinical Development, Neurocrine Biosciences, Inc., 12790 El Camino Real, San Diego, CA 92130, USA*
[d]*Department of Neuroscience, Neurocrine Biosciences, Inc., 12790 El Camino Real, San Diego, CA 92130, USA*
[e]*Department of Pediatrics, Oregon Health & Science University, Portland, OR 97239, USA*

Received 6 March 2008; revised 25 March 2008; accepted 28 March 2008
Available online 1 April 2008

Abstract—A series of 2-piperazine-α-isopropylbenzylamine derivatives were synthesized and characterized as melanocortin-4 receptor (MC4R) antagonists. Attaching an amino acid to benzylamines **7** significantly increased their binding affinity, and the resulting compounds **8**–**12** bound selectively to MC4R over other melanocortin receptor subtypes and behaved as functional antagonists. These compounds were also studied for their permeability using Caco-2 cell monolayers and metabolic stability in human liver microsomes. Most compounds exhibited low permeability and high efflux ratio possibly due to their high molecular weights. They also showed moderate metabolic stability which might be associated with their moderate to high lipophilicity. Pharmacokinetic properties of these MC4R antagonists, including brain penetration, were studied in mice after oral and intravenous administrations. Two compounds identified to possess high binding affinity and selectivity, **10d** and **11d**, were studied in a murine cachexia model. After intraperitoneal (ip) administration of 1 mg/kg dose, mice treated with **10d** had significantly more food intake and weight gain than the control animals, demonstrating efficacy by blocking the MC4 receptor. Similar in vivo effects were also observed when **11d** was dosed orally at 20 mg/kg. These results provide further evidence that a potent and selective MC4R antagonist has potential in the treatment of cancer cachexia.

1. Introduction

Cachexia, characterized by weight loss, wasting of muscle, loss of appetite, and general debility, often coincides with chronic disease states including cancer, chronic obstructive pulmonary disease, and renal failure. Cancer cachexia significantly impairs quality of life and response to anti-neoplastic therapies and ultimately increases morbidity and mortality of cancer patients. It is estimated to be responsible for over 20% of all cancer-related deaths.[1] Unfortunately, currently available drugs are not very effective.[2]

The melanocortin-4 receptor (MC4R), a member of the class A G-protein coupled receptor superfamily, is expressed in the hypothalamus, brain stem, and many other brain regions and plays a significant role in feeding behavior and energy homeostasis in animals and humans.[3] While MC4R agonists have demonstrated efficacy in suppressing food intake and reducing body

Keywords: Melanocortin-4 receptor; Antagonist; Pharmacokinetics; Cachexia; SAR.
* Corresponding author. Tel.: +1 858 617 7600; fax: +1 858 617 7602; e-mail: cchen@neurocrine.com
† Present address: Department of Medicinal Chemistry, Tanabe Research Laboratories, USA, Inc., 4540 Towne Centre Ct., San Deigo, CA 92121, USA.
‡ Present address: Vertex Pharmaceuticals Inc., 11010 Torreyana Road, San Diego, CA 92121, USA.

0968-0896/$ - see front matter © 2008 Elsevier Ltd. All rights reserved.
doi:10.1016/j.bmc.2008.03.072

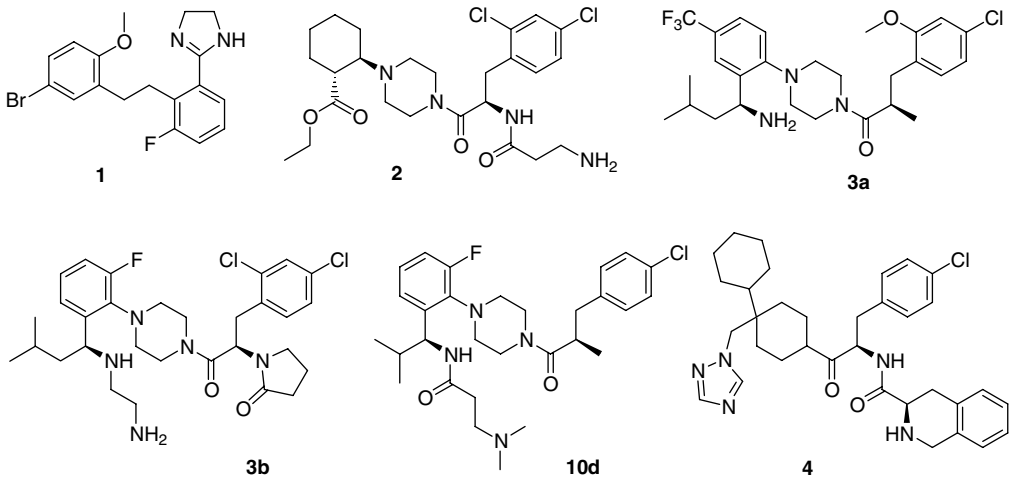

Figure 1. Chemical structures of some MC4R antagonists **1**–**3**, **10d**, and agonist **4**.

weight in animals suggesting their potential in the treatment of obesity,[4] MC4R antagonists promote food intake and increase weight gain.[5] Recent studies have demonstrated that cachexia brought about by a variety of illnesses can be attenuated or reversed by blocking MC4R activation within the central nervous system.[6]

Non-peptide MC4R antagonists have been sought and identified in recent years.[7] Because of their ability to penetrate the blood–brain barrier, small molecules with appropriate pharmacokinetic properties have been peripherally administered to demonstrate the pharmacological role of the MC4 receptor. One example is the 2-phenylimidazoline **1** (Fig. 1). After subcutaneous (sc) administration twice daily at 15 mg/kg for 13 days to C57BL6 mice-bearing tumors induced by inoculation with Lewis lung carcinoma (LLC) cells, this functional MC4R antagonist (IC_{50} = 103 nM)[8] stimulated food intake during the light-phase. During a 21-day experiment, the tumor-bearing mice treated with **1** maintained their lean body mass while vehicle-treated controls showed a reduction.[9] The binding affinity (IC_{50} = 160 nM) of this compound at MC4R is only moderate, and it might interact with the melanocortin-3 receptor which is also believed to play a role in feeding regulation.[10] We have shown that a β-alanine-2,4-dichlorophenylalanine dipeptide derivative **2** (Fig. 1) is a potent functional MC4R antagonist with negligible affinity at MC3R.[11] In addition, **2** has good brain penetration. Intraperitoneal (ip) administration of **2** effectively stimulates daytime food intake as well as decreases basal metabolic rate in normal animals. Furthermore, this compound attenuates cachexia and preserves lean body mass in a murine cancer model.[12] These data have demonstrated the potential of small molecule MC4R antagonists in the treatment of cancer cachexia.[13]

Previously, we reported the discovery of a series of piperazinebenzylamines such as **3a** (K_i = 6.5 nM) as MC4R antagonists.[14,15] While this highly lipophilic compound ($c\log P$ = 6.1) displayed metabolic instability in human liver microsomes (CL_{sys} = 17 mL/min kg), structure–activity relationship studies led to the identification of potent MC4R antagonists such as **3b** (K_i = 0.94 nM), which demonstrates efficacy in the murine cachexia model.[16] However, **3b** has low brain penetration in mice that is probably caused by its low permeability and high efflux ratio associated with its high polar surface area. Based on these leads, we started a research effort to improve their properties in several categories including potency and pharmacokinetics. Here we report the synthesis and characterization of a series of α-isopropyl benzylamine derivatives, exemplified by 1-{2-[(1*S*)-2-(1-(dimethylaminopropionyl)amino)-2-methylpropyl]-6-fluorophenyl}-4-[(2*R*)-methyl-3-(4-chlorophenyl)propionyl]piperazine (**10d**, Fig. 1), as MC4R antagonists.[§]

2. Chemistry

The target compounds **8**–**13** were synthesized from the protected piperazinebenzylamines **5**[17] as shown in Scheme 1. Compounds **5** were coupled with (2*R*)-methyl-3-(4-chlorophenyl)propionic acids[18] to give amides **6**, which were deprotected with HCl in methanol to afford benzylamines **7**. Reductive alkylation of **7** with methyl-(2-oxoethyl)carbamic acid *tert*-butyl ester provided diamines **8**–**9** after Boc-deprotection. Alternatively, coupling reactions of **7** with *N*,*N*-dimethylamino-β-alanine, or with an *N*-Boc-amino acid followed by TFA treatment, afforded **10**–**13**.

3. Results and discussion

Compounds **7**–**13** were tested for their binding affinity at the human melanocortin-4 receptor (*h*MC4R) using a binding assay as previously described,[19] and the results are summarized in Table 1. Functional antagonism was determined by their dose-dependent inhibition of α-MSH-stimulated cAMP production in CHO cells sta-

[§] Part of this work has been published as a communication, see Ref. 24.

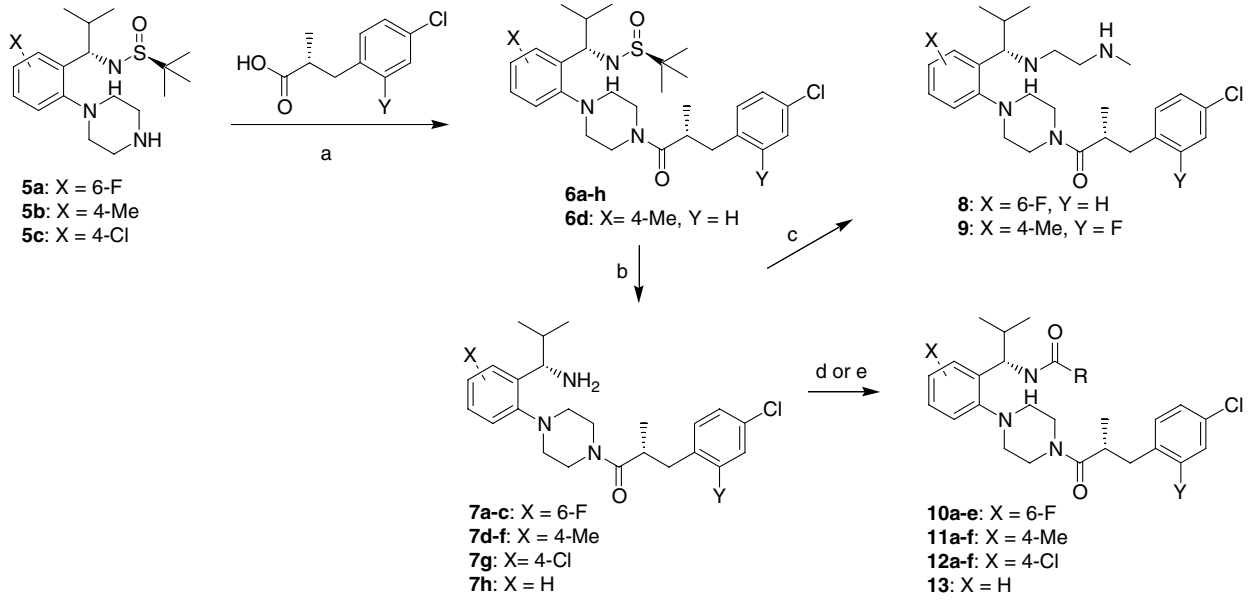

Scheme 1. Reagents and conditions: (a) i—$SOCl_2$/reflux, ii—Et_3N/CH_2Cl_2/rt, 8 h or EDC/HOBt/DIEA/DMF/rt, 3 h, 40–80%; (b) HCl/MeOH/rt, 1 h, 60–90%; (c) *N*-BocNMeCH$_2$CHO/NaBH(OAc)$_3$/CH$_2$Cl$_2$/rt, 8–14 h; then TFA/CH$_2$Cl$_2$/rt, 1–2 h, ~20%; (d) *N*-Boc-amino acid/EDC/HOBt/NaHCO$_3$/DMF/CH$_2$Cl$_2$/rt, 8 h; or HBTU/DIEA/DMF/rt, 8 h; then TFA/CH$_2$Cl$_2$/rt 1 h, 30–60%; (e) Me$_2$NCH$_2$CH$_2$COOH/EDC/HOBt/Et$_3$N/CH$_2$Cl$_2$/rt, 8 h, 70–90%.

Table 1. SAR of MC4R antagonists at the human melanocortin-4 receptor[a]

Compound	X	R	Y	K_i[b] (nM)	IC_{50}[c] (nM)
7a	6-F		H	83	n.d.[d]
7b	6-F		MeO	26	n.d.[d]
7c	6-F		Cl	27	n.d.[d]
7d	4-Me		H	69	2400
7e	4-Me		F	35	n.d.[d]
7f	4-Me		Me	9.7	n.d.[d]
7g	4-Cl		H	210	750
7h	H		H	180	n.d.[d]
8	6-F		H	23	480
9	4-Me		F	6.0	660
10a	6-F	CH_2NHMe	H	10	340
10b	6-F	CH_2NHMe	MeO	3.4	390
10c	6-F	CH_2NHMe	Cl	5.3	n.d.[d]
10d	6-F	$CH_2CH_2NMe_2$	H	7.5	270
10e	6-F	Azetadin-4-yl	MeO	3.1	42
11a	4-Me	CH_2NHMe	F	2.8	410
11b	4-Me	$CH_2CH_2NH_2$	H	5.9	280
11c	4-Me	CH_2CH_2NHMe	H	5.7	87
11d	4-Me	$CH_2CH_2NMe_2$	H	2.8	35
11e	4-Me	$CH_2CH_2NMe_2$	F	2.2	190
11f	4-Me	$CH_2CH_2NMe_2$	Me	0.6	92
12a	4-Cl	CH_2NHMe	H	4.1	300
12b	4-Cl	CH_2NHMe	MeO	1.1	290
12c	4-Cl	*R*-CH(Me)NH_2	MeO	0.8	150
12d	4-Cl	$CH_2CH_2NMe_2$	H	3.3	150
12e	4-Cl	Azetadin-4-yl	MeO	1.3	n.d.[d]
12f	4-Cl	1-Methyl-azetadin-4-yl	H	5.4	160
13	H	$CH_2CH_2NMe_2$	H	24	480

[a] Data are average of two or more independent measurements.
[b] Binding affinity was obtained using [^{125}I]NDP-MSH as the radiolabeled ligand.
[c] Dose-dependent inhibition of α-MSH-stimulated cAMP production.
[d] Not determined.

bly expressing *h*MC4R. For the binding affinity of the primary benzylamines **7a**–**c**, the 2-methoxy and 2-chloro derivatives **7b** and **7c** were much more potent than the 2-unsubstituted compound **7a**. For **7d**–**f**, the 2-methyl **7f** was about 7-fold more potent than the 2-unsubstituted analog **7d** and 4-fold more potent than the 2-fluoro **7e**.

These results indicate that a small group at the *ortho*-position of this 4-chlorophenyl group is favored, probably due to a steric effect to steer the phenyl ring to a desirable orientation for receptor interactions. In comparison, a small substituent at the left side phenyl ring had a minimal effect on binding affinity of these compounds (**7a**, **7d**, **7g**, and **7h**), only the 4-methyl compound **7d** displayed about 2-fold improvement over the non-substituted **7h**.

Incorporating a methylaminoethyl side-chain to benzylamine **7a** (K_i = 83 nM) increased the binding affinity about 4-fold (**8**, K_i = 23 nM). Similarly, a 6-fold improvement was observed for diamine **9** (K_i = 6 nM) compared to **7e**. The sarcosine derivative **10a** (K_i = 10 nM) possessed slightly higher affinity than the methylaminoethyl **8**, and this was supported by the comparison between **9** and **11a**. These results indicate that the additional amino group in **8** and **10a** is able to function as the benzylamine of **7a** to further increase affinity. The 3-(*N*,*N*-dimethylamino)propionyl derivative **10d** (K_i = 7.5 nM) was 11-fold more potent in binding affinity than its parent **7a**. Similar results were also obtained for **7d–f/11d–f**, **7g/12d**, and **7h/13** modifications. For the sarcosine derivatives **10a–c**, a chloro (**10c**) or a methoxy group (**10b**) at the 2-position of the phenyl ring in the 2*R*-methyl-3-phenylpropionyl moiety improved affinity by 2–3 times. Compound **10e**, which bears a highly basic azetadine functionality, also exhibited potent binding affinity.

Like **11d** (K_i = 2.8 nM), the *N*,*N*-dimethyl-β-alanine derivative **12d** (K_i = 3.3 nM) also possessed potent binding affinity. Compound **13** (K_i = 24 nM), however, exhibited moderate potency. None of the compounds **8–12** had significant stimulation of cAMP production at 10 μM concentration ($E_{max} \leqslant 15\%$) except **7h** (38%). All of the compounds tested in the functional antagonist assay showed dose-dependent inhibition of α-MSH-stimulated cAMP production (Table 1). For example, **11d** exhibited an IC_{50} value of 35 nM in this assay (Fig. 2). The discrepancy between the K_i and IC_{50} values is probably due to different assay conditions, however, the reason for a lack of clear correlation between these two parameters is unknown.

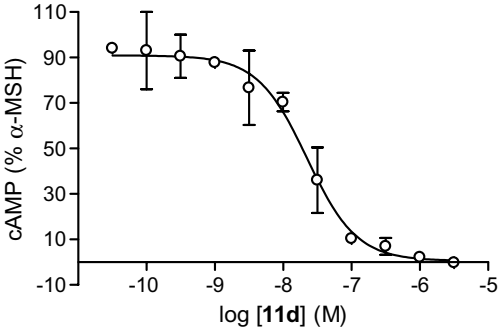

Figure 2. Functional activity of compound **11d**. (Antagonism of α-MSH-stimulated cAMP production, where 100% cAMP is defined as stimulation of cAMP production by 10 nM α-MSH (~EC_{50}) in the absence of antagonist. Assay was performed in CHO cells transfected with hMC4R, and cAMP was measured using an ELISA assay. Data are average of two independent experiments.)

Compounds **10–12** were also tested for their binding affinity at the other melanocortin receptor subtypes (Table 2). In general, these compounds had little interaction with MC1R and displayed much lower affinity at MC3R than MC4R. For example, **10d** and **11d** had over 60- and 100-fold selectivity, respectively, at MC4R over MC3R or MC5R. Several compounds (**10b**, **12b**, and **12c**) bearing a 2-methoxy-4-chlorophenylpropionyl group exhibited high binding affinity at MC5R. For example, compound **12b** had a K_i value of 13 nM at MC5R, while its binding affinity at MC4R was 1.1 nM. The wider receptor selectivity of compounds **10d** and **11d** was tested at a concentration of 10 μM in a panel of radioligand binding assays for approximately 70 receptors, ion channels, enzymes and transporters as described previously.[12] Significant activity was seen only at the ghrelin receptor with K_i values of 240 and 680 nM for **10d** and **11d**, respectively. In a functional assay, **10d** had negligible activation at the ghrelin receptor (8% stimulation at 10 μM concentration based on calcium flux). Because of the low affinity of **10d** and **11d** for the ghrelin receptor compared to MC4R (32- and 200-fold selectivity, respectively), the contribution of the ghrelin component to the actions of **10d** and **11d** should be minimal.[20] Consequently, both compounds show excellent selectivity for MC4R.

The X-ray crystal structure of **6d** was resolved (Fig. 3). In this solid state, the 4-chlorophenyl ring of **6d** was almost parallel to the piperazine ring. Interestingly, this precursor of antagonist **7d** possessed a very similar conformation to that of an MC4R agonist **4** (THIQ, Fig. 1) found in its X-ray crystal structure,[20] suggesting the framework of an antagonist structure is not much different than that of an agonist. This result indirectly indicates that the Tic-group of **4**, which is missing from antagonist **7d**, is the primary contributor to receptor activation. This conformation was further demonstrated by the X-ray crystal structure of **11e** as a mesylate salt,

Table 2. Selectivity profiles (K_i, nM) of MC4R antagonists at the human melanocortin receptor subtypes[a]

Compound	*h*MC1R[b]	*h*MC3R	*h*MC4R	*h*MC5R
10a	(49%)	570	10	1100
10b	(11%)	190	3.4	67
10d	(34%)	490	7.5	1100
11a	n.d.[c]	230	2.8	180
11b	(42%)	270	5.9	320
11c	(43%)	710	5.7	340
11d	(30%)	590	2.8	1200
12a	(28%)	200	4.1	110
12b	(19%)	160	1.1	13
12c	(40%)	220	0.8	34
12d	6200	450	3.3	390
12f	8200	380	5.4	400

[a] Data are average of two and more independent measurements.
[b] Percentage inhibition at 10 μM concentration is indicated in parentheses.
[c] Not determined.

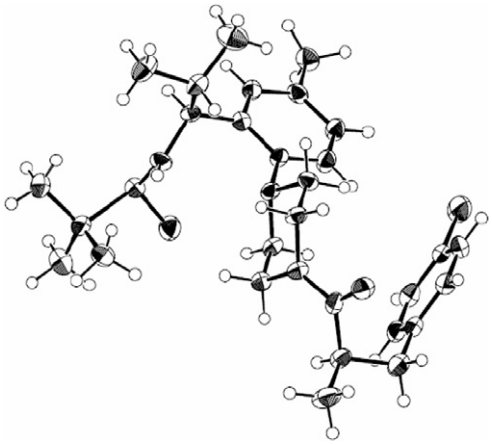

Figure 3. X-ray crystal structures of **6d**.

which possessed a similar arrangement between the 2-fluoro-4-chlorophenyl ring and the piperazine group (Fig. 4).

All of the potent compounds possessed high molecular weights (489–561). This feature presents a challenge for good oral bioavailability and brain penetration. Most of the compounds possessed moderate to high lipophilicity based on the measured log *D* values at pH of 7.4 using a shake-flask method (Table 3). These numbers matched reasonably well with the calculated values using ACD software, although for some highly basic amines such as **9** and **10e**, the difference was as high as one log unit. The measured pK_a value of *N*,*N*-dimethylaminopropionamide **11d** was 7.8, about one log unit lower than the calculated 8.9, which might explain the discrepancy for the more basic compounds. The polar surface area (PSA) for these compounds was also calculated in an attempt to correlate them with permeability.[21] Most compounds exhibited moderate values between 50 and 60 Å^2 (Table 3).

These MC4R antagonists were also tested in an in vitro Caco-2 assay measuring cell permeability and P-glycoprotein (P-gp) transporter activity, and the results are summarized in Table 4. Most compounds displayed low to moderate permeability from the apical to basolateral direction (*a* to *b*), presumably due to their high molecular weights. Many compounds had high permeability from basolateral to apical direction (*b* to *a*), indicative of an efflux mechanism due to high P-gp activity. Benzylamine **7d** showed moderate permeability

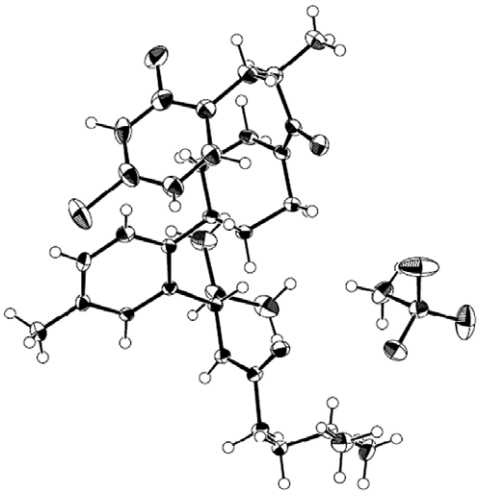

Figure 4. X-ray crystal structures of **11e** mesylate.

Table 3. Physicochemical properties of MC4R antagonists[a]

Compound	MW	log *D*[b]	*c*log *D*	*c*log *P*	pK_a	PSA (Å^2)
7d	428	n.d.[c]	2.3	4.7	9.8	50
8	489	2.6	2.0	4.5	10, 5.8	48
9	503	2.5	1.5	4.2	10, 6.2	48
10a	503	2.4	3.1	3.5	8.0	65
10b	533	3.1	3.3	3.7	8.0	74
10c	537	4.3	3.7	4.2	8.0	65
10d	531	2.4	3.4	4.4	8.9	56
10e	545	2.6	1.7	3.8	9.8	74
11a	516	4.0	2.8	3.3	8.0	65
11b	499	2.4	2.5	3.7	8.9	79
11c	513	2.7	1.9	4.0	9.6	65
11d	527	3.4	3.4	4.5	8.9[d]	56
11e	545	3.5	3.0	4.1	8.9	56
11f	541	4.0	3.9	4.9	8.9	56
12a	519	4.3	3.5	3.9	8.0	65
12b	549	3.5	3.6	4.1	8.0	74
12c	549	4.5	3.8	4.4	8.2	88
12d	547	4.0	3.7	4.7	8.9	56
12e	561	2.3	2.0	4.1	9.8	74
12f	545	3.0	3.0	4.4	9.1	56

[a] Calculated values were obtained using ACD software.
[b] Measured using a shake-flask method at pH of 7.4.
[c] Not determined.
[d] The measured pK_a value was 7.8.

Table 4. Permeability in Caco-2 cells and metabolic stability of **8**–**12**[a]

Compound	P_{app} (10^{-6} cm/s)	Efflux ratio (*b* to *a*/*a* to *b*)	CL_{sys}[c] (mL/min kg)
7d	5	3.7	13.4
8	0.4	61	13.5
9	3	26	n.d.[b]
10a	1	15.4	13.3
10b	2	8.3	16.5
10c	2	14	14.7
10d	10	4.4	11.9
10e	0.2	740	14
11a	8	7.3	12.4
11b	3	25.8	9.2
11c	12	7.2	4.8
11d	41	4.5	12.2
11e	37	3	16.1
11f	16	4.5	16.6
12a	n.d.[b]	n.d.[b]	13.1
12b	n.d.[b]	n.d.[b]	16.1
12c	3	6.9	15.5
12d	9	11	15.9
12e	0.3	120	12.3
12f	2	14.4	11.6

[a] Digoxin was used as a control in the Caco-2 assay, and it showed on average P_{app} of 1.0×10^{-6} cm/s and efflux ratio of 20–30.
[b] Not determined.
[c] Determined using human liver microsomes in an in vitro assay.

($P_{app} = 5.0 \times 10^{-6}$ cm/s) and a relatively low efflux ratio (*b* to *a*/*a* to *b* = 3.7). Methylaminoethyl **9** exhibited lower permeability and higher efflux ratio (Table 4). In comparison, the monobasic sarcosine **11a** showed an improved permeability profile compared to **9**. The 3-(*N*,*N*-dimethylamino)propionyl side-chain (**11e**), however, increased permeability from **11a**. For the three β-alanine derivatives **11b–d**, the primary amine **11b** had lowest permeability and highest efflux, while the monomethylamine **11c** displayed an improvement. The high permeability of **11d** might be associated with its high log *D* value of 3.4 and/or lower polar surface area (56 Å^2) than the secondary and primary amines **11b–c** (PSA = 65 and 79 Å^2, respectively).

When incubated with human liver microsomes in an in vitro assay, all compounds exhibited moderate metabolic stability, which might be associated in part with their high lipophilicity or/and high molecular weight (Table 4). For example, the 3-(*N*,*N*-dimethylamino)propionyl **11d** (CL_{sys} = 12.2 mL/min kg) had a much higher systemic clearance than its less lipophilic monomethyl analog **11c** (CL_{sys} = 4.8 mL/min.kg).

3.1. Pharmacokinetic properties

Compounds **8**, **10a–e**, **11a**, **11d**, and **12a–f** were studied in mice for their pharmacokinetic properties, and the results are summarized in Table 5. Whole brain concentrations were sampled at 1 and 4 h after intravenous administration in these studies. Diamine **8** had a moderate plasma clearance (CL = 36 mL/min kg) and a very large volume of distribution (V_d = 52 L/kg), which might be associated with its dibasic structure,[22] resulting in a very long half-life ($t_{1/2}$) of 17 h. Oral bioavailability (F% = 47) was good in this species. Despite its high tissue distribution, the compound had moderate whole brain concentrations (53 and 62 ng/g at 1 and 4 h postdosing, respectively), presumably due to P-gp activity impairing its penetration through the blood–brain barrier.[23] In the in vitro Caco-2 assay, **8** exhibited poor permeability ($P_{app} = 0.4 \times 10^{-6}$ cm/s) and a very high efflux ratio of 61 (Table 4), indicating strong P-gp activity. Interestingly, the calculated PSA value of 48 Å^2 was moderate. The three sarcosine derivatives **10a–c** displayed high plasma clearance (39–52 mL/min kg) and high volume of distribution (13–29 L/kg). The $t_{1/2}$ for these compounds ranged from 3.8 to 6.5 h, and their oral bioavailabilities were moderate (12–23%). The least lipophilic compound **10a** (log *D* = 2.4) had the highest brain concentrations at 1 and 4 h postdosing. The 3-(*N*,*N*-dimethylamino)propionyl **10d** had a moderate V_d of 5.2 L/kg, a short $t_{1/2}$ of 2.3 h, and penetrated into the brain with a brain/plasma (*b*/*p*) ratio of 0.6 and 0.8 at the 1 and 4 h time points, respectively. Compound **10d** also had good plasma exposure after oral administration, resulting in a 42% oral bioavailability. In contrast, the highly basic azatadine **10e** had lower brain penetration and much lower oral bioavailability compared to **10d**. In the Caco-2 assay, **10d** had a moderate P_{app} value (10×10^{-6} cm/s) and a relatively low efflux ratio (4.4) compared to P_{app} of 0.2×10^{-6} cm/s and an efflux ratio of 740 for **10e**. Therefore, the difference in permeability and P-gp activity between these two compounds might be the key determinants of their differing oral absorption and brain penetration profiles.

The 4-methylphenyl compounds **11a** and **11d** had moderate oral bioavailability but low brain penetration. Among the 4-chlorophenyl derivatives **12a–f**, **12b**, and **12d** had high brain concentrations, while **12f** had high oral bioavailability. The low permeability and high P-gp activity of **12f** may have impaired its brain penetration but not intestinal absorption. It is worth noting that the calculated PSA (56 Å^2) of **12f** was similar to that of **12d**.

Table 5. Pharmacokinetic parameters of MC4R antagonists in mice[a]

Compound	CL (mL/min kg)	V_d (L/kg)	$t_{1/2}$ (h)	C_b (ng/g) at 1, 4 h[b]	*b*/*p* ratio at 1, 4 h	T_{max} (h)	C_{max} (ng/mL)	Oral AUC (ng/mL h)	F%
8	36	52	17	53, 62	0.4, 1.2	0.5	166	1629	47
10a	42	19	5.2	231, 126	0.6, 1.1	0.5	165	813	21
10b	52	29	6.5	165, 107	0.5, 1.7	0.5	114	374	12
10c	39	13	3.8	85, 71	0.3, 0.5	2.0	172	1014	23
10d	26	5.2	2.3	322, 175	0.6, 0.8	0.5	308	2690	42
10e	28	10	4.4	51, 32	0.1, 0.4	2.0	104	336	5.6
11a	24	3	1.4	59, 42	0.1, 0.2	2	632	2290	30
11d	29.6	4.1	1.6	19, 18[c,d]	0.1, 0.1[c,e]	0.5	946	2530	32
12a	102	16	1.8	131, 62	0.7, 1.5	0.5	88	232	13
12b	69	11	1.8	334, 102	1.3, 1.3	0.5	55	208	8.0
12c	74	16	1.9	95, 59	0.4, 1.0	0.25	143	397	16
12d	64	11	1.9	580, 176	1.9, 2.3	1	109	600	19
12e	23	8.2	4.2	61, 39	0.1, 0.4	2	151	422	5.8
12f	11	3	3.2	79, 77	0.1, 0.1	6	762	9163	58

[a] Three animals were dosed intravenously at 5 mg/kg and orally at 10 mg/kg.
[b] Brain concentrations were taken from iv dose.
[c] Brain samples were taken from oral administration.
[d] Brain C_{max} = 91 ng/g, T_{max} = 0.3 h, AUC = 367 ng/g h.
[e] *b*/*p* (C_{max}) = 0.1; *b*/*p* (AUC) = 0.15.

The brain concentration versus time relationship of **11d** in mice was studied in a separate experiment. After a 10 mg/kg oral dosing, a C_{max} of 91 ng/g appeared at 0.3 h time point. The area under the curve (AUC) was 367 ng/g h (Fig. 5). The brain/plasma ratio was 0.1 based on C_{max} values or 0.15 based on AUCs. These results confirmed the finding from 1 and 4 h sampling (Table 5).

The brain concentration–time relationship of **11d** was also studied in rats after an oral administration at 10 mg/kg. The maximal whole brain concentration of **11d** was 41 ng/g at the 6 h time point, and the AUC was 254 ng/g h. The brain to plasma ratio was 0.17 based on AUC values.[24] These results were consistent with those obtained in mice for this compound.

Compounds **10d** and **11d** were studied in rats, monkeys, and dogs for their pharmacokinetic properties, and the results for **10d** are summarized in Table 6 (data for **11d** can be found in Ref. 24).

The PK profile of **10d** in rats was very similar to that of **11d**. One significant difference was the much slower brain penetration of **10d** compared to that of **11d**. The maximal brain concentration of **10d** (52 ng/g) appeared at 6 h postdosing (2.7 h for **11d**). The *b*/*p* ratio of **10d** based on AUCs (0.48) was larger than that based on C_{max} values (0.27). **10d** had a relatively large V_d value across all species (5.2–8.7 L/kg). The oral bioavailabilities of **10d** were moderate (21–42%) in these species, which were similar to that of **11d**. The half-life of **10d** was shorter in mice (2.3 h) than in dogs (7.0 h). In comparison, **11d** exhibited a similar $t_{1/2}$ of 6.7 h in dogs.

3.2. In vivo efficacy studies

We have previously established a mouse cachexia model in which the cachectic state is induced by inoculation with LLC tumor cells.[12] Compounds **2** and **3b** have demonstrated efficacy in this model in that they reverse the weight loss that is observed in the control group. Since compounds **10d** and **11d** exhibited superior pharmacological and pharmacokinetic profiles, they were also tested in this model. The binding affinity of **10d** was determined at the mouse melanocortin receptors, and it was found to bind mouse MC4R (K_i = 3.5 nM) much better than mouse MC3R (K_i = 190 nM). Similar selectivity was also demonstrated at the rat receptors (K_i = 5.5 nM for MC4R vs 340 nM for MC3R). Therefore, no species selectivity in terms of receptor affinity was observed for this compound.

For the in vivo study, C57BL/6J male mice were inoculated with Lewis lung carcinoma (LLC) tumor cells. Beginning 10 days after LLC inoculation, animals were treated over 4 days with **10d** twice daily (0.1, 1.0, or 3.0 mg/kg, ip). At 0.1 mg/kg, **10d** showed a moderate effect on food intake of tumor-bearing mice, but it was not significantly different from the control animals. However, 1 and 3 mg/kg of **10d** dose-dependently increased food intake compared with vehicle controls (Fig. 6).

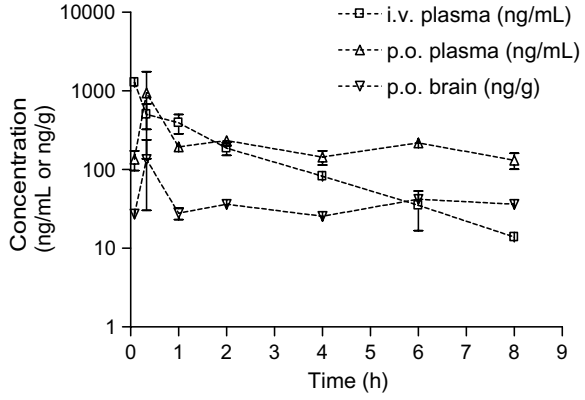

Figure 5. Time–concentration curves of **11d** in mice after iv (5 mg/kg) and po (10 mg/kg) administration.

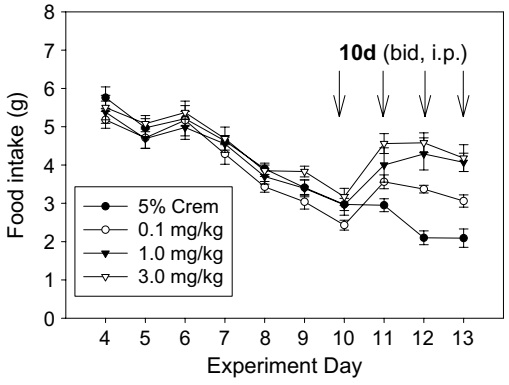

Figure 6. The effects of **10d** given twice daily (0.1, 1, and 3 mg/kg, ip) on food intake in LLC tumor-bearing mice.

Table 6. Pharmacokinetic parameters of **10d** in rats, monkeys, and dogs[a]

Species	CL (mL/min kg)	V_d (L/kg)	$t_{1/2}$ (h)	T_{max} (h)	C_{max} (ng/mL)	oral AUC (ng/mL h)	*F*%	brain AUC (ng/g h)[b]
Rat[c]	27	7.7	3.4	6	195	1290	31	618[d,e,f]
Monkey	13.8	5.6	4.7	6.7	200	2650	21	n.d.[g]
Dog	15.3	8.7	7.0	4.0	250	3850	37	n.d.[g]

[a] Three animals were dosed intravenously at 5 mg/kg and orally at 10 mg/kg.
[b] Brain concentrations were taken from po dose.
[c] The plasma protein binding of **10d** was high (>99%) in rats based on an in vitro ultrafiltration study.
[d] Brain C_{max} = 52 ng/g, T_{max} = 6.0 h.
[e] *b*/*p* = 0.27 based on C_{max} values and 0.48 based on AUCs.
[f] C_{brain} = 6.3 and 38 ng/g at 1 and 4 h, *b*/*p* ratio was 0.05 and 0.2, respectively.
[g] Not determined.

Body weight and body composition were also significantly affected in mice treated with **10d** (Fig. 7). Body weight was increased in animals treated with all doses of **10d** compared to the body weight loss (approximately 3%) which occurred in the vehicle-treated cachectic animals (Fig. 7A). Analysis of body composition with dual-energy X-ray absorbtometry (DEXA) demonstrated that the greater increase of body weight in **10d**-treated mice was probably due to the sparing of lean mass (LM). Tumor-bearing animals treated with vehicle demonstrated no increase in LM over the course of the 14-day experiment, whereas tumor-bearing animals treated with **10d** showed a trend toward an increased LM of ~4%. However, the difference between the dose groups and vehicle-treated animals was not statistically significant.

Compound **11d** was also studied in this in vivo model using oral administration. Beginning 12 days after LLC inoculation, animals were treated over 4 days with **11d** twice daily (5 or 20 mg/kg, po). LLC tumor-bearing mice treated with **11d** at a 20 mg/kg dose showed a significant increase in both food intake and weight gain relative to vehicle-treated tumor-bearing controls.[24] However, at a 5 mg/kg dose, **11d** did not have an effect on weight gain, suggesting this dose is not optimal for efficacy. Studies on the surrogate concentrations of **11d** after 20 mg/kg administration showed that the lowest concentration before the following dose was 140 ng/mL for plasma and 11 ng/g for brain (Table 7). The plasma protein binding of **11d** was 99% in rats. Assuming linear PK, a dose of 5 mg/kg po would result in a minimal brain concentration of about 2 ng/mL (~4 nM), which might be too low for high receptor occupancy (the binding affinity K_i of **11d** at mouse MC4R was 3.2 nM). This study also indicates that the compound did not accumulate in either plasma or brain after twice daily dosing in mice.

In conclusion, we conducted a detailed study on a series of α-isopropyl piperazinebenzylamines bearing an amine side-chain as MC4R antagonists. These compounds showed high binding affinity at MC4R and selectivity over other melanocortin receptor subtypes. They also functioned as antagonists by dose-dependent inhibition of α-MSH-stimulated cAMP production. These compounds were profiled in mice for their pharmacokinetic properties. Several compounds were identified to have good pharmacokinetics with moderate to high brain penetration. One analog, 1-{2-[(1*S*)-2-(1-(dimethylaminopropionyl)amino)-2-methylpropyl]-6-fluorophenyl}-4-[(2*R*)-methyl-3-(4-chlorophenyl)propionyl]piperazine (**10d**) was identified to have good potency and selectivity. It was profiled for its metabolic and pharmacokinetic properties in several animal species. Finally, this compound demonstrated efficacy in a mouse cachexia model.

4. Experimental

4.1. Chemistry

4.1.1. General Methods. NMR spectra were recorded on a Varian 300 MHz spectrometer with TMS as an internal standard. Chemical shifts are reported in parts per million (δ), and signals are expressed as s, singlet; d, doublet; t, triplet; q, quartet; m, multiplet; or br, broad.

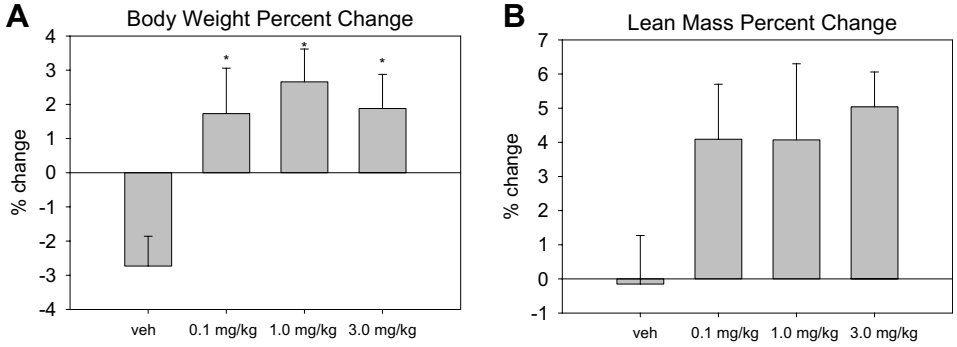

Figure 7. The effects of **10d** after 0.1, 1, and 3 mg/kg ip administration twice per day on body weight (A, left) and lean mass (B, right) in tumor-bearing mice.

Table 7. Surrogate marker of plasma concentrations of **11d** in tumor-bearing mice[a]

Time (h)	Day 1					Day 4				
	0	2	10	12	24[b]	0	2	10	12	24[c]
Dose	×		×			×		×		
C_{plasma} (ng/mL)		360		430	140		460		405	22
C_{brain} (ng/g)		27		74	11		36		25	4.5

[a] Oral administration at 20 mg/kg dose at 8:00 am and 6:00 pm each day for 4 days. Plasma and brain samples were taken from the satellite group.
[b] Samples taken before the next dose.
[c] Samples were taken 14 h after the last dose.

Purity measurements were performed on an HP Agilent 1100 HPLC–MS (detection at 220 and 254 nm).

4.1.1.1. 1-{2-[(1*S*)-(*S*-*tert*-Butylsulfinyl)amino-2-methylpropyl]-6-fluorophenyl}-4-[(2*R*)-methyl-3-(4-chlorophenyl)propionyl]piperazine (6a). 1-{2-[(1*S*)-(*S*-*tert*-Butylsulfinyl)amino-2-methylpropyl]-6-fluorophenyl}-4-(*tert*-butoxycarbonyl)piperazine (**5a**, 1.09 g, 2.4 mmol)[17] was dissolved in CH_2Cl_2 (24 mL) and trifluoroacetic acid (4.8 mL). The reaction mixture was stirred at rt for 50 min and quenched with aqueous $NaHCO_3$. The organic layer was separated, washed with saturated $NaHCO_3$, dried over anhydrous Na_2SO_4, filtered, and concentrated in vacuo. The crude product was obtained as a yellow foam (610 mg, 72%), which was dissolved in dichloromethane (24 mL). Triethylamine (1.0 mL) was added to this solution at 0 °C, followed by (*R*)-2-methyl-3-(4-chlorophenyl)propionyl chloride (obtained from 524 mg (2.64 mmol) of the corresponding acid and thionyl chloride) in CH_2Cl_2 (5 mL). The mixture was allowed to slowly warm to rt overnight and was quenched with 1 N HCl. The organic layer was separated, washed, with saturated aqueous $NaHCO_3$, dried over anhydrous $MgSO_4$, and concentrated in vacuo to yield the crude product (1.06 g), which was used in the next step without further purification. MS: 536 (MH^+).

The synthesis and characterization of compounds **6d** can be found in the supporting information of Ref. 24.

4.1.1.2. 1-{2-[(1*S*)-Amino-2-methylpropyl]-6-fluorophenyl}-4-[(2*R*)-methyl-3-(4-chlorophenyl)propionyl]-piperazine trifluoroacetate (7a). 1-{2-[(1*S*)-(*S*-*tert*-Butylsulfinyl)amino-2-methylpropyl]-6-fluorophenyl}-4-[(2*R*)-methyl-3-(4-chlorophenyl)propionyl]piperazine (**6a**, 23.3 g, 43.55 mmol) was dissolved in MeOH (436 mL) and treated with HCl (2 M in ether, 28.3 mL, 56.62 mmol). The reaction mixture was stirred at rt for about 1 h until all of the starting material had been consumed. The reaction mixture was concentrated in vacuo. The resulting yellowish foam was dried in high vacuum for 15 min to provide the crude product as an off-white foam in quantitative yield (18.8 g). A small sample was purified using an LC–MS system, and pure compound was obtained for biological studies. White solid, HPLC purity: 100% (220 and 254 nm); ^1H NMR (CD_3OD): 0.78 (d, J = 6.6 Hz, 3H), 1.16 (d, J = 6.6 Hz, 3H), 1.18 (d, J = 6.6 Hz, 3H), 2.08–2.23 (m, 1H), 2.45–3.00 (m, 5H), 3.15–3.30 (m, 4H), 4.48–4.46 (m, 2H), 4.74 (d, J = 9.7 Hz, 1H), 7.15–7.43 (m, 7H); MS: 432 (MH^+).

4.1.1.3. 1-{2-[(1*S*)-Amino-2-methylpropyl]-6-fluorophenyl}-4-[(2*R*)-methyl-3-(2-methoxy-4-chlorophenyl)-propionyl]piperazine trifluoroacetate (7b). This compound was synthesized from **5a** and (2*R*)-methyl-3-(2-methoxy-4-chlorophenyl)propionic acid using the procedure for **7a**. White foam, HPLC purity: 100% (220 and 254 nm); ^1H NMR ($CDCl_3$): 0.73 (d, J = 5.3 Hz, 3H), 1.10 (d, J = 5.3 Hz, 3H), 1.12 (d, J = 6.6 Hz, 3H), 2.03–2.20 (m, 1H), 2.50–2.80 (m, 3H), 2.80–2.97 (m, 2H), 3.05–3.28 (m, 3H), 3.58–3.66 (m, 2H), 3.73–3.96 (m, 3H), 3.80 (s, 3H), 4.50–4.70 (m, 1H), 6.92 (d, J = 6.1 Hz, 1H), 6.99 (dd, J = 1.7, 8.3 Hz, 1H), 7.08–7.20 (m, 2H), 8.12–8.48 (br s, 2H, NH_2); MS: 462 (MH^+); HRMS (MH^+) calcd for $C_{25}H_{33}ClFN_3O_2$: 462.2324; found: 462.2320.

4.1.1.4. 1-{2-[(1*S*)-Amino-2-methylpropyl]-6-fluorophenyl}-4-[(2*R*)-methyl-3-(2,4-dichlorophenyl)propionyl]piperazine trifluoroacetate (7c). This compound was synthesized from **5a** and (2*R*)-methyl-3-(2,4-dichlorophenyl)propionic acid using the procedure for **7a**. Yellowish foam, HPLC purity: 98.8% (220 nm) and 100% (254 nm); ^1H NMR 0.72 (d, J = 5.7 Hz, 3H), 1.06 (d, J = 5.7 Hz, 3H), 1.17 (d, J = 6.6 Hz, 3H), 2.03–2.20 (m, 1H), 2.46–2.90 (m, 5H), 2.92–3.30 (m, 3H), 3.50–3.90 (m, 3H), 4.47–4.70 (m, 1H), 6.87–7.07 (m, 1H), 7.08–7.21 (m, 4H), 7.35 (d, J = 8.8 Hz, 1H), 8.00–8.40 (br s, 2H, NH_2); MS: 466 (MH^+); HRMS (MH^+) calcd for $C_{24}H_{30}Cl_2FN_3O$: 466.1828; found: 466.1831.

The synthesis and characterization of compounds **7d**–**f** can be found in the supporting information of reference.[24]

4.1.1.5. 1-{2-[(1*S*)-Amino-2-methylpropyl]-4-chlorophenyl}-4-[(2*R*)-methyl-3-(4-chlorophenyl)propionyl]-piperazine trifluoroacetate (7g). This compound was synthesized from **5c** using a procedure similar to that for **7a**. White solid, HPLC purity: 100% (220 and 254 nm); ^1H NMR (CD_3OD): 0.77 (d, J = 6.6 Hz, 3H); 1.14 (d, J = 6.6 Hz, 3H), 1.20 (d, J = 6.6 Hz, 3H), 2.03–2.17 (m, 1H), 2.46–2.61 (m, 2H), 2.71–2.93 (m, 5H), 3.20–3.30 (m, 4H), 4.56 (d, J = 9.7 Hz, 1H), 7.24 (d, J = 8.3 Hz, 2H), 7.34 (d, J = 8.3 Hz, 2H), 7.40 (d, J = 2.2 Hz, 1H), 7.42–7.46 (m, 2H); MS: 448 (MH^+).

4.1.1.6. 1-{2-[(1*S*)-Amino-2-methylpropyl]phenyl}-4-[(2*R*)-methyl-3-(4-chlorophenyl)propionyl]piperazine trifluoroacetate (7h). This compound was synthesized from **5d** using a procedure similar to that for **7a**. White solid, HPLC purity: 98.4% (220 nm) and 100% (254 nm); ^1H NMR (CD_3OD): 0.75 (d, J = 6.6 Hz, 3H), 1.15 (d, J = 6.6 Hz, 3H), 1.20 (d, J = 6.6 Hz, 3H), 2.05–2.21 (m, 2H), 2.46–2.62 (m, 2H), 2.63–2.93 (m, 5H), 3.20–3.32 (m, 3H), 4.59 (d, J = 9.7 Hz, 1H), 7.20–7.50 (m, 8H); MS: 414 (MH^+). HRMS (MH^+) calcd for $C_{24}H_{32}ClN_3O$: 414.2312; found: 414.2310.

4.1.1.7. 1-{2-[(1*S*)-(Methylaminoethyl)amino-2-methylpropyl]-6-fluorophenyl}-4-[(2*R*)-methyl-3-(4-chlorophenyl) propionyl]piperazine mesylate (8). Sodium triacetoxyborohydride (510 mg, 2.4 mmol) was added to a stirred solution of 1-{2-[(1*S*)-amino-2-methylpropyl]-6-fluorophenyl}-4-[(2*R*)-methyl-3-(2-fluoro-4-chlorophenyl)propionyl]piperazine (**7a**, 280 mg, 0.60 mmol) and methyl-(2-oxoethyl)carbamic acid *tert*-butyl ester (135 mg, 0.78 mmol) in dichloromethane (6 mL), and the reaction mixture was stirred at rt for 8 h. An aqueous workup provided a crude intermediate which was dissolved in 1:1 trifluoroacetic acid/CH_2Cl_2 (6 mL), and the solution was stirred at rt for 2 h. The crude product was concentrated in vacuo and purified on a LC–MS system to give the titled compound as a TFA salt, which was neutralized with Na_2CO_3 to provide a free amine (50 mg, 17% yield), which was converted into the mesylate salt

(57 mg). White powder, HPLC purity: 98.7% (220 nm) and 95.1% (254 nm); ^{1}H NMR ($CDCl_3$): 0.77 (m, 3H), 1.18 (m, 6H), 2.10 (m, 1H), 2.55–3.35 (m, 16H), 2.68 (s, 3H, $MeSO_3$), 2.79 (s, 3H), 3.77 (m, 1H), 4.43 (m, 1H), 4.62 (d, J = 12 Hz, 1H), 7.01 (m, 1H), 7.13 (dd, J = 1.8, 8.1 Hz, 1H), 7.25 (s, 4H), 7.26 (m, 1H); MS: 489 (MH^+). Anal. Calcd for $C_{27}H_{38}ClFN_4O{\cdot}MeSO_3H{\cdot}1/2H_2O$: C, 54.93%; H, 7.41%; N, 9.15%. Found: C, 54.62%; H, 7.34%; N, 9.15%.

The synthesis and characterization of compounds **9** can be found in the supporting information of Ref. 24.

4.1.1.8. 1-{2-[(1*S*)-(Methylaminoacetamido)-2-methylpropyl]-6-fluorophenyl}-4-[(2*R*)-methyl-3-(4-chlorophenyl) propionyl]piperazine mesylate (10a). HBTU (292 mg, 0.77 mmol) was added to a solution of *N*-Boc-sarcosine (104 mg, 0.55 mmol) and DIEA (440 μL) in DMF (6 mL). The mixture was stirred at rt for 30 min, and 1-{2-[(1*S*)-amino-2-methylpropyl]-6-fluorophenyl}-4-[(2*R*)-methyl-3-(2-fluoro-4-chlorophenyl)propionyl]piperazine (**7a**, 233 mg, 0.50 mmol) was added, followed by 3 mL of DMF. The reaction mixture was stirred at rt for 8 h. After an aqueous workup, the mixture was dissolved in TFA/CH_2Cl_2 (1:1, ~5 mL) and stirred at rt for 1 h. After concentration in vacuo, the product was purified by chromatography on silica gel with 400:50:2 $CHCl_3$/MeOH/NH_4OH to give the titled compound as a free amine (80 mg, 32% yield), which was converted to the mesylate salt. White powder, HPLC purity: 97.6% (220 nm) and 95% (254 nm); ^{1}H NMR ($CDCl_3$): 0.75 (m, 3H), 1.01 (m, 3H), 1.16 (m, 3H), 1.98 (m, 1H), 2.69 (s, 6H, 3H for $MeSO_3$), 2.60-3.40 (m, 9H), 3.85 (m, 3H), 4.61 (m, 1H), 5.33 (m, 1H), 6.92 (m, 1H), 7.15 (br s, 4H), 7.27 (m, 2H), 8.41 (br s, 3H); MS: 503 (MH^+). Anal. Calcd for $C_{27}H_{36}ClFN_4O_2{\cdot}MeSO_3H{\cdot}7/2H_2O$: C, 50.79%; H, 7.15%; N, 8.46%. Found: C, 51.07%; H, 7.09%; N, 8.58%.

4.1.1.9. 1-{2-[(1*S*)-(Methylaminoacetamido)-2-methylpropyl]-6-fluorophenyl}-4-[(2*R*)-methyl-3-(2-methoxy-4-chlorophenyl)propionyl]piperazine mesylate (10b). This compound was synthesized from **7b** using the procedure for **10a**. White powder, HPLC purity: 99.0 (220 nm) and 93.6% (254 nm); ^{1}H NMR (DMSO-d_6): 0.73 (d, J = 6.3 Hz, 3H), 0.99 (d, J = 6.3 Hz, 6H), 1.86 (m, 1H), 2.30 (s, 3H), 2.57 (m, 1H), 2.78 (s, 3H), 2.76–2.79 (m, 1H), 3.15 (m, 4H), 3.69 (m, 1H), 3.78 (m, 1H), 3.82 (s, 3H), 3.94 (m, 1H), 4.41 (m, 1H), 5.34 (m, 1H), 6.92 (d, J = 8.1 Hz, 1H), 7.00–7.15 (m, 4H), 7.23 (m, 1H), 8.61 (br s, 2H), 8.77 (d, J = 8.1 Hz, 1H); MS:533 (MH^+); HRMS (MH^+) calcd for $C_{28}H_{38}ClFN_4O_3$: 533.2695; found: 533.2681.

4.1.1.10. 1-{2-[(1*S*)-(Methylaminoacetamido)-2-methylpropyl]-6-fluorophenyl}-4-[(2*R*)-methyl-3-(2,4-dichlorophenyl)propionyl]piperazine mesylate (10c). This compound was synthesized from **7c** using the procedure for **10a**. Light yellow foam, HPLC purity: 99.1% (220 nm) and 97.6% (254 nm); ^{1}H NMR (CD_3OD): 0.75 (d, J = 7.0 Hz, 3H), 1.03 (d, J = 6.6 Hz, 3H), 1.20 (d, J = 6.6 Hz, 3H), 1.88–2.02 (m, 1H), 2.56 (s, 3H, $MeSO_3$), 2.50–2.60 (m, 1H), 2.60–2.70 (m, 1H), 2.80–3.10 (m, 6H), 3.34–3.66 (m, 4H), 3.20–3.32 (m, 3H), 3.84–3.94 (m, 1H), 4.47 (d, J = 9.7 Hz, 1H), 6.91–7.01 (m, 1H), 7.04–7.10 (m, 1H), 7.15–7.22 (m, 1H), 7.27 (s, 1H), 7.22–7.29 (m, 1H), 7.43–7.48 (m, 1H); MS: 537 (MH^+); HRMS (MH^+) calcd for $C_{27}H_{35}Cl_2FN_4O_2$: 537.2199; found: 537.2213.

4.1.1.11. 1-{2-[(1*S*)-(3-Dimethylaminopropionamino)-2-methylpropyl]-6-fluorophenyl}-4-[(2*R*)-methyl-3-(4-chlorophenyl)propionyl]piperazine mesylate (10d). The crude 1-{2-[(1*S*)-amino-2-methylpropyl]-6-fluorophenyl}-4-[(2*R*)-methyl-3-(4-chlorophenyl)propionyl]piperazine (**7a**, ~18.8 g, ~43.5 mmol) was dissolved in dichloromethane (218 mL) along with 3-dimethylaminopropionic acid hydrochloride (7.36 g, 47.91 mmol) and diisopropylethylamine (30.3 mL, 174.2 mmol). The reaction mixture was stirred at rt for 5 min then HOBt (8.82 g, 65.33 mmol) was added. After 40 min, EDC (4.73 g, 24.67 mmol) was added to the reaction mixture, and stirring was continued for an additional 2 h. The reaction mixture was washed with saturated aqueous $NaHCO_3$ (2× 250 mL) and brine (250 mL). The organic layer was collected, dried over anhydrous $MgSO_4$, filtered, and evaporated in vacuo to give a tan oil. The product was purified by column chromatography on silica gel using 3–10% methanol in ethyl acetate, then 90:9.5:0.5 $CHCl_3$/MeOH/NH_4OH as the eluent to give a white foam (30 g, 87% yield) as the free amine.

This amine (7.0 g, 13.18 mmol) was dissolved in ethyl acetate (40 mL) along with methanesulfonic acid (0.855 mL, 13.18 mmol), and the solution was stirred at rt for 1 h and then evaporated to dryness in vacuo. The resulting solid was dissolved in water (~60 mL), filtered, and lyophilized for 2 days to give a hygroscopic white solid (7.7 g). HPLC purity: 100% (220 nm) and 98.9% (254 nm); ^{1}H NMR ($CDCl_3$, free base): 0.86 (d, J = 6.6 Hz, 3H), 0.93 (d, J = 6.9 Hz, 3H), 1.17 (d, J = 6.6 Hz, 3H), 1.86 (m 1H), 2.31 (m, 1H), 2.35 (s, 6H), 2.50–3.40 (m, 12H), 3.80 (m, 1H), 4.65 (d, J = 12 Hz, 1H), 5.40 (m, 1H), 6.84 (d, J = 8.1 Hz, 1H), 6.90 (m, 1H), 7.12 (m, 3H), 7.26 (m, 2H), 9.11 and 9.21 (d, J = 9.0 Hz, 1H); MS: 531 (MH^+). Anal. Calcd for $C_{29}H_{40}ClFN_4O_2{\cdot}MeSO_3H{\cdot}3H_2O$: C, 52.89%; H, 7.40%; N, 8.22%. Found: C, 53.09%; H, 7.64%; N, 8.50%.

4.1.1.12. 1-{2-[(1*S*)-(3-Azetidinylcarboxamido)-2-methylpropyl]-6-fluorophenyl}-4-[(2*R*)-methyl-3-(2-methoxy-4-chlorophenyl)propionyl]piperazine mesylate (10e). This compound was synthesized from **7b** and *N*-Boc-azetidine-3-carboxylic acid using a procedure similar to that for **10a**. White powder, HPLC purity: 98.6% (220 nm) and 100% (254 nm); ^{1}H NMR ($CDCl_3$): 0.74 (m, 3H), 1.02 (m, 3H), 1.13 (m, 3H), 2.02 (m, 1H), 2.69 (s, 3H), 2.60–3.25 (m, 5H), 3.35 (m, 2H), 3.83 (s, 3H), 3.91 (m, 1H), 4.25 (m, 4H), 4.63 (m, 1H), 5.22 (m, 1H), 6.82–7.24 (m, 6H), 8.06 (br s, 1H), 8.56 (br s, 1H), 8.93 (br s, 1H); MS:545 (MH^+); HRMS (MH^+) calcd for $C_{29}H_{38}ClFN_4O_3$ 545.2695; found: 545.2681.

The synthesis and characterization of compounds **11a**–**f** can be found in the supporting information of Ref. 24.

4.1.1.13. 1-{2-[(1*S*)-(Methylaminoacetamido)-2-methylpropyl]-4-chlorophenyl}-4-[(2*R*)-methyl-3-(4-chlorophenyl) propionyl]piperazine dimesylate (12a). This compound was synthesized from **7g** using a procedure similar to that for **10a**. White powder, HPLC purity: 100% (220 and 254 nm): ^{1}H NMR (DMSO-d_6, free amine): 0.68 (d, J = 6.9 Hz, 3H), 0.95 (d, J = 6.3 Hz, 3H), 1.04 (d, J = 6.6 Hz, 3H), 1.79 (m, 1H), 2.28 (m, 1H), 2.35(s, 3H), 2.46 (m, 2H), 2.54 (m, 2H), 2.63 (m, 1H), 2.82 (dd, J = 8.7, 12.9 Hz, 1H), 3.18 (br s, 2H), 3.30–3.88 (m, 4H), 5.14 (m, 1H), 7.01 (d, J = 8.7 Hz, 1H), 7.26 (m, 3H) 7.35 (m, 3H), 8.64 (br s, 1H), 8.80 (d, J = 8.4 Hz, 1H); MS: 519 (MH^+). Anal. Calcd for $C_{27}H_{36}Cl_2N_4O_2{\cdot}2MeSO_3H{\cdot}3/2CH_2Cl_2.2H_2O$: C, 41.86%; H, 5.87%; N, 6.40%. Found: C, 41.63%; H, 5.68%; N, 7.15%.

4.1.1.14. 1-{2-[(1*S*)-(Methylaminoacetamido)-2-methylpropyl]-4-chlorophenyl}-4-[(2*R*)-methyl-3-(2-methoxy-4-dichlorophenyl)propionyl]piperazine dimesylate (12b). This compound was synthesized from 1-{2-[(1*S*)-amino-2-methylpropyl]-4-chlorophenyl}-4-[(2*R*)- methyl-3-(2-methoxy-4-chlorophenyl)propionyl]piperazine using a procedure similar to that for **10a**. HPLC purity: 100% (220 and 254 nm); ^{1}H NMR (DMSO-d_6, free amine): 0.69 (d, J = 6.3 Hz, 3H), 0.95 (d, J = 6.6 Hz, 3H), 1.00 (d, J = 6.6 Hz, 3H), 1.80 (m, 1H), 2.34 (s, 3H), 2.56 (m, 1H), 2.58 (m, 1H), 2.73 (dd, J = 7.2, 9.9 Hz, 1H), 3.16 (m, 2H), 3.80 (m, 2H), 3.84 (s, 3H), 4.40 (br s, 6H), 5.17 (t, J = 9.0Hz, 1H), 6.95 (dd, J = 1.8, 7.8 Hz, 1H), 7.04 (d, J = 8.7 Hz, 1H), 7.08 (m, 2H), 7.26 (dd, J = 2.1, 8.7 Hz, 1H), 7.33 (d, J = 2.4 Hz, 1H), 8.62 (br s, 1H), 8.80 (d, J = 9.0 Hz, 1H); MS: 549 (MH^+). Anal. Calcd for $C_{28}H_{38}Cl_2N_4O_3{\cdot}2MeSO_3H{\cdot}CH_2Cl_2$: C, 45.04%; H, 5.85%; N, 6.78%. Found: C, 45.02%; H, 5.54%; N, 7.00%.

4.1.1.15. 1-{2-[(1*S*)-((2*R*)-Aminopropionamido)-2-methylpropyl]-4-chlorophenyl}-4-[(2*R*)-methyl-3-(2-methoxy-4-dichlorophenyl)propionyl]piperazine mesylate (12c). This compound was synthesized from 1-{2-[(1*S*)-amino-2-methylpropyl]-4-chlorophenyl}-4-[(2*R*)-methyl-3-(2-methoxy-4-chlorophenyl)propionyl]piperazine and *N*-Boc-D-alanine using a procedure similar to that for **10a**. White solid, HPLC purity: 97.6% (220 nm) and 96.9% (254 nm); ^{1}H NMR (CD_3OD, TFA salt): 0.73 (d, J = 6.6 Hz, 3H), 1.01 (d, J = 6.6 Hz, 3H), 1.15 (d, J = 6.6 Hz, 3H), 1.56 (d, J = 7.0 Hz, 3H), 1.80–1.95 (m, 1H), 2.42–2.55(m, 2H), 2.66–2.87 (m, 3H), 3.10–3.28 (m, 3H), 3.28–3.40 (m, 1H), 3.58–3.66 (m, 1H), 3.88 (s, 3H), 3.80–3.96 (m, 2H), 5.31 (d, J = 9.2 Hz, 1H), 6.91 (dd, J = 2.2, 10.1 Hz, 1H), 6.88–6.98 (m, 1H), 7.03–7.09 (m, 2H), 7.20 (dd, J = 2.2, 8.3 Hz, 1H), 7.30(d, J = 2.6 Hz, 1H); MS: 549 (MH^+); HRMS (MH^+) calcd for $C_{28}H_{38}Cl_2N_4O_3$: 549.2399; Found: 549.2401.

4.1.1.16. 1-{2-[(1*S*)-(3-Dimethylaminopropionamino)-2-methylpropyl]-4-chlorophenyl}-4-[(2*R*)-methyl-3-(4-chlorophenyl)propionyl]piperazine mesylate (12d). This compound was synthesized from **7g** using the procedure for **10d**. White powder, HPLC purity: 98.6% (220 nm) and 97.4% (254 nm); ^{1}H NMR (DMSO-d_6): 0.66 (d, J = 6.3 Hz, 3H), 0.91 (d, J = 6.3 Hz, 3H), 1.02 (d, J = 6.6 Hz, 3H), 1.78 (m, 1H), 2.35–2.90 (m, 6H), 2.72 (s, 6H), 3.05–3.65 (m, 9H), 5.08 (m, 1H), 6.98 (m, 1H), 7.18–7.42 (m, 6H), 8.48 (d, J = 8.4 Hz, 1H); MS: 547 (MH^+). Anal. Calcd for $C_{29}H_{40}Cl_2N_4O_2{\cdot}MeSO_3H{\cdot}H_2O$: C, 54.46%; H, 7.01%; N, 8.47%. Found: C, 54.52%; H, 7.47%; N, 8.67%.

4.1.1.17. 1-{2-[(1*S*)-(Azetidine-3-carboxamido)-2-methylpropyl]-4-chlorophenyl}-4-[(2*R*)-methyl-3-(2-methoxy-4-dichlorophenyl)propionyl]piperazine dimesylate (12e). This compound was synthesized from 1-{2-[(1*S*)-amino-2-methylpropyl]-4-chlorophenyl}-4-[(2*R*)-methyl-3-(2-methoxy-4-chlorophenyl)propionyl]piperazine and *N*-Boc-azetidine-3-carboxylic acid using a procedure similar to that for **10a**. White powder, HPLC purity: 97% (220 nm) and 95% (254 nm); ^{1}H NMR (DMSO-d_6): 0.68 (d, J = 6.3 Hz, 3H), 0.92 (d, J = 6.6 Hz, 3H), 1.00 (d, J = 6.6 Hz, 3H), 1.78 (m, 1H), 2.27 (m, 1H), 2.58 (m, 1H), 2.74 (m, 1H), 3.16 (m, 2H), 3.25–4.18 (m, 11H), 3.85 (s, 3H), 5.14 (t, J = 9.0 Hz, 1H), 6.95 (dd, J = 1.8, 7.8 Hz, 1H), 7.02 (d, J = 8.4 Hz, 1H), 7.09 (m, 2H), 7.25 (dd, J = 2.4, 8.7 Hz, 1H), 7.29 (d, J = 2.1 Hz, 1H), 8.46 (d, J = 8.7 Hz, 1H), 8.63 (br s, 1H); MS: 561 (MH^+). Anal. Calcd for $C_{29}H_{38}Cl_2N_4O_3{\cdot}2MeSO_3H{\cdot}CH_2Cl_2$: C, 45.83%; H, 5.77%; N, 6.68%. Found: C, 45.58%; H, 5.72%; N, 6.78%.

4.1.1.18. 1-{2-[(1*S*)-(1-Methyl-3-azetadinylcarbonyl)-amino-2-methylpropyl]-4-chlorophenyl}-4-[(2*R*)-methyl-3-(4-chlorophenyl)propionyl]piperazine mesylate (12f). A solution of 1-{2-[(1*S*)-(3-azetadinylcarbonyl)amino-2-methylpropyl]-4-chlorophenyl}-4-[(2*R*)-methyl-3-(4-chlorophenyl)propionyl]piperazine (154 mg, 0.29 mmol), synthesized from **7g** and *N*-Boc-azetidine-3-carboxylic acid using a procedure similar to that for **10a**, and formaldehyde (37% in water, 3 drops, excess) in methanol (3 mL) was treated with sodium cyanoborohydride (100 mg, 1.5 mmol) portionwise. The mixture was stirred at rt for 0.5 h and diluted with water (2 mL). The product was extracted with ethyl acetate (2 × 20 mL), and the combined extract was dried over Na_2SO_4, filtered, and concentrated in vacuo. Chromatography on silica gel using $CHCl_3$/MeOH/NH_4OH (200:25:1) gave the product (69 mg, 44% yield) as a free base which was converted to the mesylate salt using 1 equiv of methanesulfonic acid in dichloromethane. White powder, HPLC purity: 100% (220 nm) and 98% (254 nm); ^{1}H NMR ($CDCl_3$, free base): 0.78 (d, J = 6.6 Hz, 3H), 0.98 (d, J = 6.3 Hz, 3H), 1.19 (d, J = 5.7 Hz, 3H), 1.88 (m, 1H), 2.32 (s, 3H), 2.44 (m, 1H), 3.00 (m, 5H), 3.10–3.68 (m, 9H), 5.14 (t, J = 8.7 Hz, 1H), 6.92 (d, J = 7.5 Hz, 1H), 6.99 (d, J = 8.7 Hz, 1H), 7.05–7.30 (m, 4H), 7.28 (d, J = 7.8 Hz, 2H); MS: 545 (MH^+). Anal. Calcd for $C_{29}H_{38}Cl_2N_4O_2{\cdot}MeSO_3H{\cdot}2H_2O$: C, 53.17%; H, 6.84%; N, 8.27%. Found: C, 53.20%; H, 6.43%; N, 8.37%.

4.1.1.19. 1-{2-[(1*S*)-(3-Dimethylaminopropionyl) amino-2-methylpropyl]phenyl}-4-[(2*R*)-methyl-3-(4-chlorophenyl)propionyl]piperazine trifluoroacetate (13). This compound was synthesized from **7h** using the procedure for **10d**. Yellowish solid, HPLC purity: 100% (220 nm); ^{1}H NMR (CD_3OD): 0.71 (d, J = 7.0 Hz, 3H), 1.00 (d,

J = 6.6 Hz, 3H), 1.20 (d, J = 6.6 Hz, 3H), 1.77–1.84 (m, 1H), 2.41–2.50 (m, 2H), 2.85 (s, 6H), 2.60–2.94 (m, 6H), 3.05–3.30 (m, 4H), 3.30–3.37 (m, 2H), 3.60–3.70 (m, 1H), 5.30 (d, J = 8.8 Hz, 1H), 6.88–7.00 (m, 1H), 7.13 (dd, J = 0.9, 7.5 Hz, 1H), 7.19 (dd, J = 1.8, 7.5 Hz, 1H), 7.21–7.29 (m, 3H), 7.30–7.37 (m, 2H); MS: 513 (MH^+); HRMS (MH^+) calcd for $C_{29}H_{41}ClN_4O$: 513.2996, found: 513.3008.

4.2. Pharmacology

Receptor binding was performed on membranes from HEK293 cells stably expressing the human melanocortin receptors, using [^{125}I]NDP-MSH as the radiolabeled ligand. The cAMP stimulation and inhibition assays were performed in the same cell lines using α-MSH (as the standard in agonist assay). The assay conditions were similar to those previously reported.[19]

4.3. Pharmacokinetic characterization

The pharmacokinetic profiles of selected compounds were determined in animals (N = 3/time points at a dose of 10 mg/kg for po or 5 mg/kg for iv). Compounds were dosed as a mesylate salt in 5% methylcellulose via the tail vain (iv) or in water with 5% v/v cremophor via oral gavage (po). Composite sampling was used to collect samples. Terminal blood samples were taken from treated mice at nine time points ranging from pre-dose to 24 h (0, 0.25, 0.5, 1, 2, 4, 6, 8, and 24 h) postdose. Brain samples were collected at 1 and 4 h post po dosing in rats for all compounds. Brain samples were also collected at 0, 0.25, 0.5, 1, 2, 4, 6, 8, and 24 h post po dosing in mice and rats for compound **10d**.

Plasma and brain sample analyses for the quantification of parent compounds were conducted using a HPLC equipped with a mass spectrometric detector (LC–MS/MS). For plasma samples, the compound was extracted via a protein precipitation assay by adding 130 mL of acetonitrile (CAN) and 30 mL of internal standard in 50 μL of mouse plasma (EDTA). Standards and QCs were prepared by drying 50 mL of spiked aqueous solutions and reconstituting with 50 mL of blank mouse plasma. For brain samples, the whole brain was homogenized in 2.0 mL of ACN/H_2O/formic acid (v/v, 60:40:0.1) containing 50 mL of internal standard, and the supernatant was collected and injected into an LC–MS/MS system for analysis. Brain standards and QCs were prepared by adding 1.0 mL of spiked aqueous solutions (prepared in 60:40 ACN/H_2O), 1.0 mL of ACN/H_2O/formic acid (v/v: 60:40:0.1), and 50 mL of internal standard into a whole blank mouse brain. Standards and QCs for both plasma and brain were processed and analyzed at the same time and in exactly the same way as the analytical samples. The compound was measured using a specific and sensitive HPLC/MS assay that offered linear ranges of 1–1000 ng/mL for iv/po plasma sample analysis, and 1–500 ng/mL for iv brain sample analysis. The lower limit of quantitation (LLOQ) was 1 ng/mL for the study. Quantification for both plasma and brain samples was performed by fitting peak area ratios to a weighted (1/×) linear calibration curve.

Descriptive pharmacokinetics were derived and evaluated based on the mean plasma concentrations (N = 3/time point). A non-compartmental model in ActivityBase with linear trapezoidal rule was used to perform all pharmacokinetic analyses pertaining to this manuscript.

4.4. Efficacy study

C57BL/6J male mice obtained from Jackson Laboratories (Bar Harbor, Maine) were used for the cachexia studies. Mice were housed individually and maintained on powdered Purina 5015 chow (13% fat) for at least seven days prior to the start of the study. All studies were conducted according to the NIH Guide for the Care and Use of Laboratory Animals and approved by the Animal Care and Use Committee of the Oregon Health Sciences.

As previously described,[3] on day 0, mice were inoculated subcutaneously into the upper flank with 1×10^6 cells from a subcloned Lewis lung carcinoma (LLC) cell line. All experimental animals were found to have a palpable tumor within five days of the start of the experiment. At the time of sacrifice, tumors were dissected away from the surrounding tissue and weighed. There was no statistical difference in tumor size between treatment groups, and gross examination of organs did not reveal the presence of metastasis.

On day 10 after tumor inoculation, mice were divided into four groups and treated twice daily with vehicle, 0.1, 1.0, 3.0 mg/kg **10d** (ip). Food intake and body weight were measured daily. Following 4 days of treatment, animals were sacrificed, tumors were removed and body composition was determined by dual-energy X-ray absorbtometry (DEXA, PIXImus mouse densitometer, Lunar Corp.). A baseline measure was made on the day of inoculation (day 0) also. Animals were anesthetized prior to the first scan and asphyxiated with CO_2 prior to the tumor dissection and the final scan.

Food intake was averaged over the treatment days. Percent change in body weight, lean mass, and fat mass was computed from the initial day of the experiment to the final day. Differences among groups for these variables were analyzed by one-way ANOVAs with post hoc analysis. Data sets were analyzed for statistical significance using SigmaStat (SPSS, Inc).

Acknowledgment

The authors are indebted to Mr. Andrew Fisher for the technical support in Caco-2 assay and liver microsomes stability measurements

References and notes

1. Gordon, J. N.; Green, S. R.; Goggin, P. M. *Qjm* **2005**, *98*, 779–788.
2. Bossola, M.; Pacelli, F.; Tortorelli, A.; Doglietto, G. B. *Ann. Surg. Oncol.* **2007**, *14*, 276–285.
3. Cone, R. D. *Trends Endocrinol. Metab.* **1999**, *10*, 211–216.

4. Boyce, R. S.; Duhl, D. M. *Curr. Opin. Investig. Drugs* **2004**, *5*, 1063–1071.
5. Foster, A. C.; Joppa, M.; Markison, S.; Gogas, K. R.; Fleck, B. A.; Murphy, B. J.; Wolff, M.; Cismowski, M. J.; Ling, N.; Goodfellow, V. S.; Chen, C.; Saunders, J.; Conlon, P. J. *Ann. NY Acad. Sci.* **2003**, *994*, 103–110.
6. DeBoer, M. D.; Marks, D. L. *Nat. Clin. Pract. Endocrinol. Metab.* **2006**, *2*, 459–466.
7. Foster, A. C.; Chen, C. *Curr. Top. Med. Chem.* **2007**, 1131–1136.
8. Vos, T. J.; Caracoti, A.; Che, J. L.; Dai, M.; Farrer, C. A.; Forsyth, N. E.; Drabic, S. V.; Horlick, R. A.; Lamppu, D.; Yowe, D. L.; Balani, S.; Li, P.; Zeng, H.; Joseph, I. B.; Rodriguez, L. E.; Maguire, M. P.; Patane, M. A.; Claiborne, C. F. *J. Med. Chem.* **2004**, *47*, 1602–1604.
9. Nicholson, J. R.; Kohler, G.; Schaerer, F.; Senn, C.; Weyermann, P.; Hofbauer, K. G. *J. Pharmacol. Exp. Ther.* **2006**, *317*, 771–777.
10. Marks, D. L.; Cone, R. D. *Ann. NY Acad. Sci.* **2003**, *994*, 258–266.
11. Tucci, F. C.; White, N. S.; Markison, S.; Joppa, M.; Tran, J. A.; Fleck, B. A.; Madan, A.; Dyck, B. P.; Parker, J.; Pontillo, J.; Arellano, L. M.; Marinkovic, D.; Jiang, W.; Chen, C. W.; Gogas, K. R.; Goodfellow, V. S.; Saunders, J.; Foster, A. C.; Chen, C. *Bioorg. Med. Chem. Lett.* **2005**, *15*, 4389–4395.
12. Markison, S.; Foster, A. C.; Chen, C.; Brookhart, G. B.; Hesse, A.; Hoare, S. R.; Fleck, B. A.; Brown, B. T.; Marks, D. L. *Endocrinology* **2005**, *146*, 2766–2773.
13. Foster, A. C.; Chen, C.; Markison, S.; Marks, D. L. *IDrugs* **2005**, *8*, 314–319.
14. Jiang, W.; Tucci, F. C.; Chen, C. W.; Arellano, M.; Tran, J. A.; White, N. S.; Marinkovic, D.; Pontillo, J.; Fleck, B. A.; Wen, J.; Saunders, J.; Madan, A.; Foster, A. C.; Chen, C. *Bioorg. Med. Chem. Lett.* **2006**, *16*, 4674–4678.
15. Chen, C. W.; Tran, J. A.; Jiang, W.; Tucci, F. C.; Arellano, M.; Wen, J.; Fleck, B. A.; Marinkovic, D.; White, N. S.; Pontillo, J.; Saunders, J.; Madan, A.; Foster, A. C.; Chen, C. *Bioorg. Med. Chem. Lett.* **2006**, *16*, 4800–4803.
16. Jiang, W.; Tucci, F. C.; Tran, J. A.; Fleck, B. A.; Wen, J.; Markison, S.; Marinkovic, D.; Chen, C. W.; Arellano, M.; Hoare, S. R.; Johns, M.; Foster, A. C.; Saunders, J.; Chen, C. *Bioorg. Med. Chem. Lett.* **2007**, *17*, 5610–5613.
17. Jiang, W.; Chen, C.; Marinkovic, D.; Tran, J. A.; Chen, C. W.; Arellano, L. M.; White, N. S.; Tucci, F. C. *J. Org. Chem.* **2005**, *70*, 8924–8931.
18. Tran, J. A.; Jiang, W.; Tucci, F. C.; Fleck, B. A.; Wen, J.; Sai, Y.; Madan, A.; Chen, T.; Markison, S.; Foster, A. C.; Hoare, S. R.; Marks, D.; Harman, J.; Chen, C. W.; Marinkovic, D.; Bozigian, H.; Saunders, J.; Chen, C. *J. Med. Chem.* **2007**, *50*, 5356–5366.
19. Nickolls, S. A.; Cismowski, M. I.; Wang, X.; Wolff, M.; Conlon, P. J.; Maki, R. A. *J. Pharmacol. Exp. Ther.* **2003**, *304*, 1217–1227.
20. (a) Sebhat, I. K.; Martin, W. J.; Ye, Z.; Barakat, K.; Mosley, R. T.; Johnston, D. B.; Bakshi, R.; Palucki, B.; Weinberg, D. H.; MacNeil, T.; Kalyani, R. N.; Tang, R.; Stearns, R. A.; Miller, R. R.; Tamvakopoulos, C.; Strack, A. M.; McGowan, E.; Cashen, D. E.; Drisko, J. E.; Hom, G. J.; Howard, A. D.; MacIntyre, D. E.; van der Ploeg, L. H.; Patchett, A. A.; Nargund, R. P. *J. Med. Chem.* **2002**, *45*, 4589–4593; (b) Mutulis, F.; Yahorava, S.; Mutule, I.; Yahorau, A.; Liepinsh, E.; Kopantshuk, S.; Veiksina, S.; Tars, K.; Belyakov, S.; Mishnev, A.; Rinken, A.; Wikberg, J. E. *J. Med. Chem.* **2004**, *47*, 4613–4626.
21. Pagliara, A.; Reist, M.; Geinoz, S.; Carrupt, P.; Testa, B. *J. Pharm. Pharmacol.* **1999**, *51*, 1339–1357.
22. Bjorkman, S. *J. Pharm. Pharmacol.* **2002**, *54*, 1237–1245.
23. Fromm, M. F. *Trends Pharmacol. Sci.* **2004**, *25*, 423–429.
24. Chen, C.; Jiang, W.; Tucci, F. C.; Tran, J. A.; Fleck, B. A.; Hoare, S. R.; Joppa, M.; Markison, S.; Wen, J.; Sai, Y.; Johns, M.; Madan, A.; Chen, T.; Chen, C. W.; Marinkovic, D.; Arellano, M.; Saunders, J.; Foster, A. C. *J. Med. Chem.* **2007**, *50*, 5249–5252.